PCCP

PAPER

View Article Online
View Journal | View Issue

Cite this: *Phys. Chem. Chem. Phys.*, 2014, **16**, 5326

Reaction-induced phase separation in a bisphenol A-aniline benzoxazine–*N*,*N*′-(2,2,4-trimethylhexane-1,6-diyl)bis(maleimide)–imidazole blend: the effect of changing the concentration on morphology†

Zhi Wang, Qichao Ran, Rongqi Zhu and Yi Gu*

Received 24th November 2013,
Accepted 18th January 2014

DOI: 10.1039/c3cp54960g

www.rsc.org/pccp

The effect of the concentration changes on morphology was researched by modulating the molar ratio of bisphenol A-aniline benzoxazine (BA-a) and *N*,*N*′-(2,2,4-trimethylhexane-1,6-diyl)bis(maleimide) (TBMI); the relationships between the concentration changes, the curing rate, rheological properties, and morphologies of blends were examined in this paper. The cured blends showed different morphologies at different concentrations, and the morphologies changed from a sea-island structure to a bi-continuous structure followed by a homogeneous structure when the molar ratio of BA-a was decreased. This effect was caused by the relative rates of the phase separation and the curing reaction. Meanwhile, from the thermodynamic calculations, it was found that the concentration changes altered the Gibbs free energy, while the miscibility of blends improved after decreasing the BA-a content. Moreover, from the analysis and the Flory–Huggins equation, it was found that the phase separation of BA-a–TBMI–imidazole occurred due to the molecular weights of the components and the large discrepancy between those weights.

Introduction

Thermoset (TS) resin is a kind of material that possesses many desirable characteristics including good thermal properties, great mechanical properties and fine processability. Unfortunately, the brittleness of this type of material precludes its use in numerous fields, including the aerospace field. Therefore, improving the toughness of TS is important to researchers. Previously, rubber-modified TS showed improved toughness sacrificing the stiffness significantly. Consequently, much work has been performed to modify the toughness of TS with thermoplastics (TP), such as polyetherimide (PEI),[1,2] which has a high modulus and glass transition temperature. However, the improved toughness resulting from this method is accompanied by a slight decrease in the quality of the thermal properties and a consequent loss in processability due to the poor thermal properties and high molecular weight of TP. Using one type of TS to improve the toughness of another type of TS is a new idea.[3,4] In this scenario, the improved toughness is due to the immiscible phase morphology caused by reaction-induced phase separation. Generally, reaction-induced phase separation is involved in several transformations,[5–7] including the phase separation processes resulting from the increased molecular weight, vitrification and/or gelation. Therefore, the cross-linking and phase separation processes control the phase morphology. Specifically, the phase morphology was determined by the rate of the cross-linking and phase separation processes. The former causes the increase of the molecular weight and the entire system to move to the thermodynamic instability position, whereas the latter is activated by the curing reaction and later suppressed by the slowing of the molecular movement. The competition between the curing reaction and the phase separation kinetics would generate different morphologies. In particular, for the TS–TS blend, the relative curing rate of the two different TS components is another important factor that influences the phase morphology.[4] Nearly the same curing reaction rate of two TS components makes the entire system thermodynamically unstable because they have nearly the same molecular weight. Therefore, the entire system becomes homogeneous. Consequently, studying the phase separation process is more complex for TS–TS blends. Therefore, studies relating these factors are critical and beneficial for controlling the morphology of TS–TS blends.

Compared to the rubber–TS and TP–TS systems, using the TS–TS system to improve the toughness maintains the thermal properties and the processability of the TS simultaneously due to excellent thermal properties and the small molecular weight

State Key Laboratory of Polymeric Materials Engineering, College of Polymer Science and Engineering, Sichuan University, Chengdu 610065, China. E-mail: guyi@scu.edu.cn; Fax: +86 28 85400377; Tel: +86 28 85400377

† Electronic supplementary information (ESI) available. See DOI: 10.1039/c3cp54960g

of the TS. Previous research on the influence of the initial curing temperature[4] and the curing sequences[8] of the components on the phase separated structures in a bisphenol A-aniline benzoxazine (BA-a)–*N*,*N*′-(2,2,4-trimethylhexane-1,6-diyl)bis(maleimide) (TBMI) blend was carried out by our group. The relative curing rates can be modified by changing the initial curing temperature, and the curing sequences of the two components can be adjusted by using different catalysts. These two factors affect the changes in the thermodynamic asymmetry, directly influencing the phase separated structures formed in the BA-a–TBMI blend. If the initial curing temperature is high enough (160 °C), a homogenous morphology is observed; if the initial curing temperature is low (120 °C), a bi-continuous morphology is obtained. The curing sequence also has an obvious effect. TBMI reacted first can generate a phase separated structure and *vice versa*. Although these two factors facilitate control over the phase separated structures in the TS–TS blend, further research and discussion regarding other factors that can influence the phase separated structures in the TS–TS blend are still needed to further control the process and the morphology.

However, the changes in the concentrations of the two components have an obvious influence over the phase separated structures in a traditional reaction-induced phase separation system, particularly in TP–TS blends. Park *et al.*[9] studied the phase separation behavior and the morphology of polyetherimide (PEI) modified diglycidyl ether of bisphenol A (DGEBA) epoxy. They observed a sea-island morphology at 10 wt% PEI modified epoxy, a nodular structure above 25 wt% PEI content and a dual phase morphology with PEI contents between 15 and 20 wt%. Li[10] added a series of PEI into the epoxy to study the phase separation mechanism and found that after the content of PEI exceeds a certain weight fraction, a phase inversion structure can be obtained. Besides PEI/epoxy, Li[11,12] studied the effect of the polyethersulfone (PES) content on the PES–epoxy system. The research showed that a sea-island morphology can be obtained in a 14 wt% PES modified epoxy, and a phase inversion structure can be observed at 20 wt% PES. The effect of the concentration changes observed in the TP–TS system may also be present in the TS–TS blends.

To control the morphology of TS–TS blends, different concentrations of BA-a/TBMI/imidazole were studied in this paper. The relationships between the concentration change, the curing rate, rheology and morphology were studied. Moreover, the effect of concentration changes on morphology was discussed based on thermodynamic calculations.

Experimental

Materials

Bisphenol A, aniline, aqueous formaldehyde solution, imidazole(I), toluene, acetone, maleic anhydride and ethyl alcohol were provided by Chengdu Kelong Chemical Reagents Corp. (China). Toluene sulfonic acid was obtained from Shanghai QianFeng Chemical Co. LTD. (China). Trimethylhexamethylenediamine was purchased from Shanghai BaoMan Biotechnology Corp. (China).

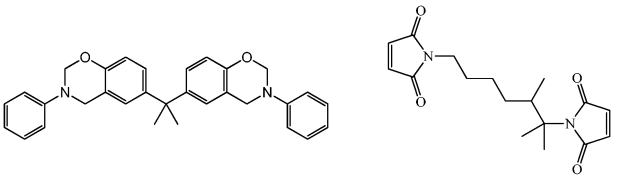

Scheme 1 Chemical structures of BA-a and TBMI.

The bisphenol A-aniline benzoxazine monomer (BA-a, mp 113 °C) was synthesized and purified according to previously described procedures.[13] *N*,*N*′-(2,2,4-trimethylhexane-1,6-diyl)bis-(maleimide) (TBMI, mp 88 °C) was synthesized and purified in our laboratory following a reported procedure.[14] The structures of BA-a and TBMI are shown in Scheme 1.

Preparation of the blended sample

BA-a was blended with TBMI in a 1/1 molar ratio (BA-a/TBMI) at 110 °C for 10 min before being cooled to 25 °C. Subsequently, imidazole, with 3 wt% of the blend dissolved in acetone was added into the blend and the mixture was stirred for 10 min. This blend is defined as BTI113, where B represents BA-a, T represents TBMI and I represents imidazole. Besides, the BTI213 and BTI123 (molar ratios of BA-a to TBMI are 2/1 and 1/2, and the amount of imidazole is also 3 wt% of the blend) were prepared as stated above. Afterward, different blends were cast into an aluminum plate and degassed under vacuum at 60 °C for 1 h before being transferred to a metal mold. The casts were cured with the following profile: 120 °C/4 h, 160 °C/4 h, and 200 °C/2 h.

Measurements

The morphology of the cured sample and the evolution of phase separation in the blends were observed by field emission-scanning electron microscopy (FESEM) with an FEI Inspect F. The samples were fractured in liquid nitrogen, and some of the samples were etched in tetrahydrofuran (THF) at room temperature for 1 h (unless indicated, the samples were not etched in THF). Then, the fractured surfaces were coated with gold and observed with an accelerating voltage of 20 KV.

The phase morphology of the cured blend was also investigated by transmission electron microscopy (TEM) using a JSM-7500F apparatus. The sample was microtomed at room temperature using a Leica EMFCS instrument equipped with a diamond knife. The resulting ultrathin section (100 nm thick) was placed on a copper grid to observe phase morphology with an accelerating voltage of 80 KV.

The curing behavior was studied using differential scanning calorimetry (DSC) performed on a TA Instrument DSC-Q20. The non-isothermal tests for BTI213 and BTI113 were conducted at 10 °C min^{-1}, and the isothermal tests were conducted at 120 °C to obtain the time-conversion curves. The conversion, α,[15] was calculated as $\alpha = H_t/H_u$ where H_t is the reaction heat within time t, H_u is the total heat of reaction (H_u is the sum of the H_i and H_r, where H_i is the heat obtained from the isothermal curing measurements, and H_r is the residual heat obtained by

scanning the samples again at 10 °C min^{-1} after the isothermal curing measurements). All of the DSC tests were performed under nitrogen at a flow rate of 50 ml min^{-1}.

An AR-G2 rheometry instrument was used to record the variations in the melt viscosity of the blends during the curing reaction. Approximately 1 g of the blend was sandwiched between two round plates 20 mm in diameter and softened at 100 °C for 1 min. The plate distance was adjusted to 0.8 mm, and the temperature was raised quickly to 120 °C at 120 °C min^{-1}. All blends were tested in parallel plate mode with a controlled strain of 1%, and the frequency of the test was 1 rad s^{-1}.

Results and discussion

The morphology of different blends

Fig. 1 shows the FESEM images of the fracture surface of BTI213, BTI113 and BTI123. As observed from Fig. 1a, some spheroid particles were dispersed in the matrix with clear boundaries. The size of the island structure ranged from 1–3 μm and had a narrow size distribution. These phenomena indicate that a sea-island structure is formed in BTI213. In contrast to BTI213, a bi-continuous structure is formed in BTI113, as shown in Fig. 1b and described in a previous report.[3] After the concentration was changed to that of BTI123, a smooth fracture surface was clearly observed in Fig. 1c, and some river like structures were observed. These features may be generated by the internal stress formed during the curing process. Therefore, further experiments are needed to confirm the morphology of BTI123.

To observe the phase morphology, TEM was used to investigate the phase morphology of different blends. A sea-island structure and a bi-continuous structure in BTI213 and BTI113 were clearly observed in Fig. 2, respectively. In BTI213 (Fig. 2a), the island structure (light part) is composed of polymerized TBMI and the sea structure (dark part) is composed of polymerized BA-a, as explained in previous reports.[3] In the fracture surface of BTI113 (Fig. 2b), the light and dark parts were interlocked and entangled with a clear boundary. The bi-continuous structure of the cured BTI113 could be confirmed using this observation. When the concentration changed to BTI123, the whole surface shows no obvious change in the bright-dark distribution. The surface has no boundary, as observed in Fig. 2c. From the TEM results, we can conclude that a sea-island structure is formed in BTI213, a bi-continuous structure is formed in BTI113 and a homogeneous structure is formed in BTI123.

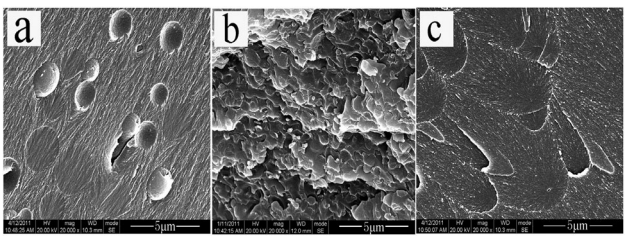

Fig. 1 FESEM images of the BA-a–TBMI–imidazole blends ((a) BTI213; (b) BTI113; (c) BTI123).

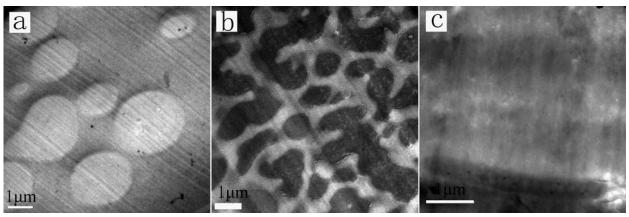

Fig. 2 TEM images of the BA-a–TBMI–imidazole blends ((a) BTI213; (b) BTI113; (c) BTI123).

The morphology evolution of different blends

Research on the phase separation process can reveal a method for controlling the phase morphology and is critical to understanding the truth of morphology. As shown in Fig. 3, a clear transformation from the homogeneous to phase separated structure occurred for BTI213. After curing at 120 °C for 50 min, the fractured surface of BTI213 was homogeneous, and no phase separation was observed, as shown in Fig. 3A. However, spheroid particles emerged after curing at 120 °C for 60 min (Fig. 3B), even though the boundary was not obvious. When the curing time was prolonged (Fig. 3C), the particles became increasingly obvious. To observe the phase morphology more clearly, the cured samples were etched in THF. As observed in Fig. 3D–F, the particle size increased with curing temperature and time. After curing at 160 °C for long time (Fig. 3G and H), the sea-island structure can still be observed, but the boundary of phase morphology was blurred, and the sample cannot be etched because of the high conversion of BA-a and TBMI. Fig. 3 indicates that the cloud point of BTI213 was located between 50 and 60 min at 120 °C, and the sea-island structure emerged at the beginning of phase separation.

In contrast to the phase separation process observed for BTI213, BTI113 exhibited bi-continuous phase morphology during the initial stages of phase separation, as shown in a previous report;[3] the cloud point of BTI113 was in the range of 60–80 min at 120 °C.[3]

The relationships between the phase separation process, the curing rate and rheological properties

Examining the relationships between the phase separation process, the curing rate and rheology properties can elucidate

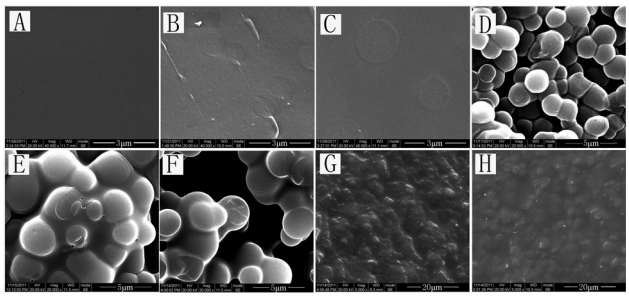

Fig. 3 FESEM images of BTI213 cured for different amounts of time at different temperatures. ((A) 120 °C/50 min; (B) 120 °C/60 min; (C) 120 °C/80 min; (D) 120 °C/180 min; (E) 120 °C/4 h and reached 160 °C; (F) 120 °C/4 h, 160 °C/30 min; (G) 120 °C/4 h, 160 °C/1 h; (H) 120 °C/4 h, 160 °C/90 min).

the details of the phase separation. The conversion and the rheological properties of BTI213 at 120 °C are shown in Fig. 4. As shown in Fig. 4A, the conversion of BTI213 ranges from 0.15 to 0.17 at the cloud point (120 °C, located between 3000 and 3600 s, as shown in Fig. 3). After curing at 120 °C for 110 min, the conversion of BTI213 reached nearly 0.25 and exhibited little change in morphology after curing time. However, the gel time (T_{gel}) for TS represents the time needed to form the three dimensional net, indicating that movement of the polymer chain is forbidden and that the morphology is fixed. The T_{gel} can be determined using the cross point of the storage (G') and loss moduli (G'') from the rheological measurements. As observed in Fig. 4B, the T_{gel} for BTI213 at 120 °C is 5200 s, and the conversion at this point is nearly 0.22, as observed in Fig. 4A.

From Fig. 3, 4A and B, it is can be seen that the phase separation occurred before gelation in BTI213 at 120 °C. The fluidity of BTI213 is good, and the polymer can move freely with the kinetic driving force when the thermodynamic state is unstable. More importantly, the fluidity of BTI213 can be maintained for a long time because of the large discrepancy between the cloud point and T_{gel} (the cloud point is located between 3000 and 3600 s at 120 °C, however the T_{gel} is 5200 s at this temperature). After curing at 120 °C for more than 5200 s, the morphology is partly fixed, and further changes in morphology may result from the local movement of macromolecular chains of two components, as shown in Fig. 3E–H.

Using the same method to study the relationship of BTI113 is convenient when comparing different blends. The conversion and rheological properties of BTI113 at 120 °C are shown in Fig. 5. At the cloud point (120 °C, located between 3600 and 4800 s, as previously reported[3]), the conversion for BTI113 was 0.25–0.37, as shown in Fig. 5A. When cured at 120 °C for 170 min, the conversion reached 0.55, and no additional changes occurred with longer curing times. As observed from the rheological data in Fig. 5B, the T_{gel} of BTI113 was 5600 s at 120 °C, and the conversion was 0.4, as observed in Fig. 5A.

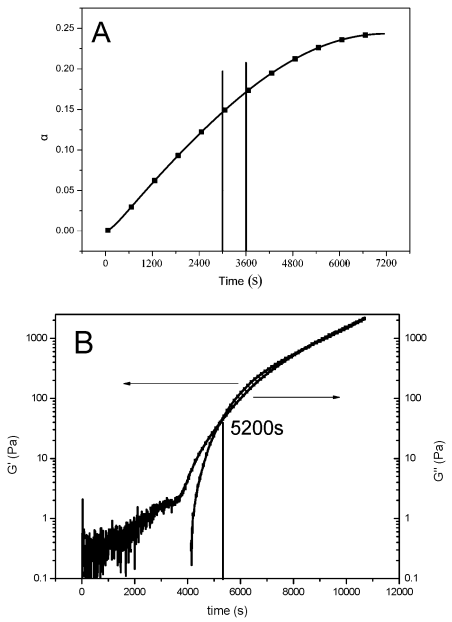

Fig. 4 Conversion *vs.* time curve (A) and the rheological behaviour (B) of BTI213 at 120 °C.

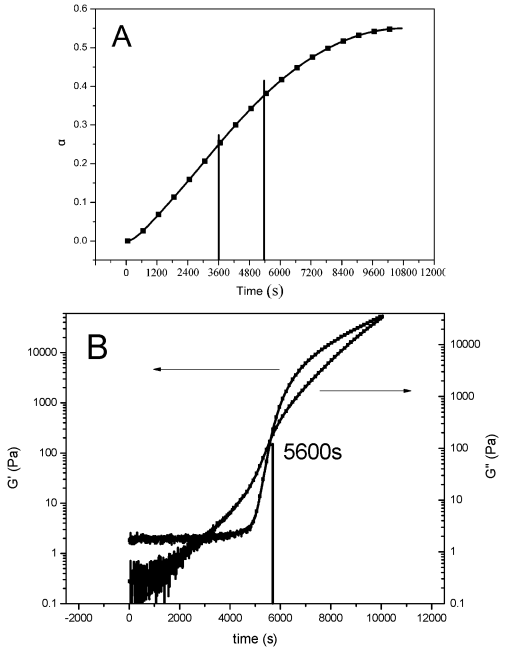

Fig. 5 Conversion *vs.* time curve (A) and rheological behaviour (B) of BTI113 at 120 °C.

Fig. 5A and B show that the cloud point was near the T_{gel}. Therefore, little time remained for phase separation, and gelation occurred immediately. BTI113 cannot become fluid without limits, and the primary method of forming morphology is the local movement of the molecular chain.

For BTI213 and BTI113, the cloud point emerged before gelation, and the entire system is fixed when gelation occurred. Therefore, the most likely reason for BTI123 forming a homogeneous structure is that the reaction rate is so fast that T_{gel} is reached before phase separation (120 °C, T_{gel} is 3800 s (Fig. S1, ESI†)). Different ratios in the BTI system show different phase separation and curing reaction rates, which potentially explain the different phase morphologies observed.

Thermodynamics of the phase separation during the curing of blends

The effects of concentration changes on the phase separation have been shown above and explained. To understand the effects of concentration changes, the thermodynamics of different blends during phase separation must be discussed. Unstable thermodynamics are required for phase separation in the BTI system.

The Flory–Huggins theory is a well-known thermodynamic equation for mixing and phase separation[16] because it defines the change in the Gibbs free energy for mixing (eqn (1)):

$$\Delta F_M = \frac{RTV}{V_s}\left[\frac{\phi}{x_A}\ln\phi + \frac{1-\phi}{x_B}\ln(1-\phi) + \chi_1\phi(1-\phi)\right] \quad (1)$$

where R is the gas constant, T is the absolute temperature, V is the volume of materials, and V_s is the reference volume. x_A and x_B represent the degrees of polymerization (actual number of repeating units) of A and B. ϕ is the volume fraction of BA-a, and χ_1 is the Flory–Huggins interaction parameter. The Flory–Huggins interaction parameter, χ_1, can be estimated by the method developed by Hildebrand and Scott,[17] which is applicable at room temperature:

$$\chi_1 = \frac{V_{ref}(\delta_i - \delta_j)^2}{RT} \quad (2)$$

where R is the gas constant, T is the absolute temperature, δ_i is the solubility parameter, and V_{ref} is the reference volume. The solubility parameters δ_i and δ_j are determined *via* group contribution methods that involve the total individual functional group contributions for different components of the structural groups.[18] The reference volume V_{ref} is the mean molar volume of the repeating unit for different polymers, as stated in eqn (3):

$$V_{ref} = \frac{M_a/\rho_a/ + M_b/\rho_b}{2} \quad (3)$$

where M_a and M_b are the molar masses of different components, and ρ_a and ρ_b are the densities of different components measured according to GBT15223-2008.

The density results for different components are $\rho_{PBA\text{-}a}$ = 1.1645 g cm^{-3} and ρ_{PTBMI} = 1.2066 g cm^{-3}. The reference volume V_{ref} = 327.627 cm^3 mol^{-1}. The value of χ_1 at room temperature is 0.6424.[4] In practice, the interaction parameter, χ, should decrease when the temperature increases[19] *via* $\chi = A + B/T$, meaning that the value of χ_1 at 120 °C is lower than that at room temperature.

The second derivative of the free energy gives the spinodal and therefore the critical interaction parameter for phase separation, which is expressed as

$$\chi_{1c} = \frac{1}{2}\left(\frac{1}{x_a^{\frac{1}{2}}} + \frac{1}{x_b^{\frac{1}{2}}}\right)^2 \quad (4)$$

where x_a and x_b represent the degrees of polymerization (actual number of repeating units) of a and b. The value of χ_{1c} decreases when the molecular weight increases. The blends are miscible if χ_1 is smaller than χ_{1c}.

In this paper, the thermoset monomers can be simplified as a component or solvent at the early stage of phase separation; therefore, before phase separation, x_a and x_b are equal to 1. After the reaction reaches the high conversion, the degree of polymerization approaches infinity. Therefore, the value of χ_{1c} is limited to (0, 2).

After curing at 120 °C, the $\chi_1 < \chi_{1c}$ at the initial state represents the initial homogeneity of the blends. After an increase in the molecular weight, χ_{1c} decreases. When $\chi_1 > \chi_{1c}$, phase separation may occur in the BTI system. When comparing the value of χ_1 with that of χ_{1c} in the BTI system, all three concentration blends might undergo phase separation in the context of thermodynamics. However, why does phase separation occur in only the BTI213 and BTI113 systems? To answer this question, the sign of ΔF_M for BTI is calculated:

If set,

$$x_b = Nx_a \quad (5)$$

where x_a and x_b are the degrees of polymerization (actual number of repeating units) for BA-a and TBMI. N is the positive real number. After incorporating eqn (5) into eqn (1), we can obtain eqn (6), as shown below:

$$\Delta F_M = \frac{RTV}{Nx_a V_s}[N\phi \ln\phi + (1-\phi)\ln(1-\phi) + \chi_1 Nx_a\phi(1-\phi)] \quad (6)$$

where all parameters are defined above. As can be seen in eqn (6), ΔF_M can be obtained by multiplying $\frac{RTV}{Nx_aV_s}$ and [$N\phi$ lnϕ + (1 − ϕ) ln(1 − ϕ) + $\chi_1 Nx_a\phi(1-\phi)$]. The $\frac{RTV}{Nx_aV_s}$ is always positive, so the sign of ΔF_M is determined by the sign of [$N\phi$ lnϕ + (1 − ϕ) ln(1 − ϕ) + $\chi_1 Nx_a\phi(1-\phi)$]. Therefore, we can change the sign of eqn (6) by moving $\frac{RTV}{Nx_aV_s}$ to the left side to obtain eqn (7).

$$\Delta F_M' = [N\phi \ln\phi + (1-\phi)\ln(1-\phi) + \chi_1 Nx_a\phi(1-\phi)] \quad (7)$$

where $\Delta F_M' = \Delta F_M \frac{RTV}{Nx_aV_s}$ and other parameters are defined as shown above. In eqn (7), $\Delta F_M'$ and ΔF_M have the same sign and $\Delta F_M'$ is determined by three factors. The first factor is the discrepancy in the degree of polymerization, another word is the discrepancy in molecular weight, N. The second factor is the polymerization degree of BA-a, x_a. The last factor is the critical interaction parameter, χ_1.

To determine the exact relationship between the concentration and ΔF_M, we examined the relationship between Nx_a and $\Delta F_M'$. Considering the system at the cloud point will help us to find the connection between Nx_a and $\Delta F_M'$ easily. As is known, the initial point of phase separation is the cloud point; the entire system remains at a critical point when the thermodynamics begins to destabilize, and χ_{1c} is equal to χ_1. Further reactions will cause χ_{1c} to become smaller than χ_1, and phase separation will occur. At this point, χ_1 $(0.6424)^4$ can be incorporated into eqn (7) to obtain eqn (8).

$$\Delta F_M' = [N\phi \ln\phi + (1-\phi)\ln(1-\phi) + 0.6424 Nx_a\phi(1-\phi)] \quad (8)$$

where all parameters are defined as shown above. Eqn (8) indicates that the sign of $\Delta F_M'$ is only related to Nx_a at certain concentrations. Therefore, the values of N and x_a at different concentrations were listed using an exhaustive method, and the corresponding sign of $\Delta F_M'$ was assessed, as shown in Table 1.

Using BTI213 as an example to illustrate the relationship between the values N, x_a and $\Delta F_M'$ in Table 1. When the degree of polymerization from TBMI to BA-a, N, equals 1, the $\Delta F_M'$ is smaller than 0 for all values of x_a. Therefore, when the components in BTI213 have the same degree of polymerization, the thermodynamic compatibility is excellent, and the system is

Table 1 Different values of N, x_a and the corresponding sign of $\Delta F_M'$

System	N	x_a	Sign of $\Delta F_M'$ Positive (P) or negative (N)
BTI213	1	—	N
	2	15.6	P
	3	2.36	P
BTI113	1	—	N
	2	—	N
	3	2.38	P
BTI123	1	—	N
	2	—	N
	3	3.006	P

stable, thus precluding phase separation. When N equals 2 and x_a is larger than 15.6, the $\Delta F_M'$ is larger than 0 (the N value is determined by an exhaustive method. The x_a value is calculated when N determined and the system is at a critical point, that is, $\Delta F_M'$ is equal to 0). Consequently, the two components have discrepancies in their degrees of polymerization; when the degree of polymerization for BA-a reaches 15.6, BTI213 is unstable in the context of thermodynamics, generating a tendency toward phase separation. When N grows to 3, x_a is only needed to be more than 2.36, causing $\Delta F_M'$ to exceed 0. Therefore, when the discrepancy becomes large, the entire system can become unstable when the degree of polymerization for BA-a is small.

Table 1 indicates that when N equals 3, x_a (polymerization degree of BA-a) becomes increasingly large as the TBMI content increases, thus destabilizing the system ($\Delta F_M'$ is positive). However, based on research by Gu,[4] BA-a is difficult to polymerize at 120 °C. Therefore, phase separation might become increasingly difficult when the TBMI content increases.

The parameters obtained using this exhaustive method were incorporated into eqn (8), and the curve for $\Delta F_M'$ *vs.* concentration was drawn, as shown in Fig. 6. As shown, the abscissa represents the content of BA-a, and the ordinate represents the value of $\Delta F_M'$. When the content of BA-a increases, the sign of $\Delta F_M'$ changes from negative to positive. Therefore, when the amount of BA-a increases, the system destabilizes from a thermodynamic perspective.

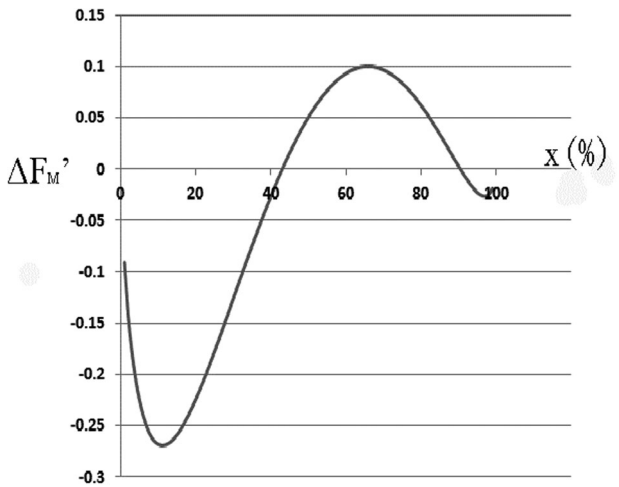

Fig. 6 Relationship between $\Delta F_M'$ and concentration change.

Based on the above explanation, we conclude that in the BTI system, changes in concentration influence the phase separation; the phase separation is hindered by increased TBMI content. Moreover, molecular weight increment of two components and discrepancies in the degree of polymerization of the two components lead to phase separation. Finally, Fig. 6 shows some points that need to be illustrated. First, $\Delta F_M'$ is not the true value because χ_1, which was taken in eqn (8), is not the true value (the true value is smaller than that used) of the system at 120 °C. However, this treatment method is adequate when only observing changes in the system for looking the tendency only. Second, it should be emphasized that $\Delta F_M'$ is different from $\Delta F_M'$. These two parameters only have the same sign. Therefore, the value of $\Delta F_M'$ shown in Fig. 6 has no meaning except with respect to the observed trends. Third, the N value cannot increase without limits because TBMI limits the degree of polymerization at 120 °C. Therefore, during the discussion in this paper, we do not need to assess additional N values because the trends can be observed through the present discussion.

Conclusions

The influence of concentration changes in BTI on phase separation was studied. Changing the content of the components can generate a sea-island structure, a bi-continuous structure and homogeneous products. The relationships between the curing rate, rheological properties and phase separation were discussed, and the influence of the concentration change on morphology was discussed based on a thermodynamic analysis. When the TBMI content increased, the curing rate was accelerated, and the cloud point neared the gel point, enabling the phase separation time to decrease. Therefore, when the TBMI content reached a certain threshold, phase separation was restrained by gelation. Moreover, based on the thermodynamic calculations, the blends tended to form a homogeneous structure because the Gibbs free energy tended to fall below 0 when TBMI increased; the conditions required for phase separation in the BTI system involved increased molecular weights and a large discrepancy in the degree of polymerization of the two components.

Acknowledgements

This work is supported by the National Natural Science Foundation of China (Project No.51273119 and No. 50873062).

Notes and references

1 A. Bonnet, J. P. Pascault, H. Sautereau, M. Taha and Y. Camberlin, *Macromolecules*, 1999, **32**, 8517.

2 C. C. Riccardi, J. Borrajo, R. J. J. Williams, E. Girard-Reydet, H. Sautereau and J. P. Pascault, *J. Polym. Sci., Part B: Polym. Phys.*, 1996, **34**, 349.
3 Z. Wang, Q. Ran, R. Zhu and Y. Gu, *RSC Adv.*, 2013, **3**, 1350.
4 Z. Wang, Z. Zhang, Q. Ran, R. Zhu and Y. Gu, *RSC Adv.*, 2013, **3**, 14029.
5 P. K. Chan and A. D. Rey, *Macromolecules*, 1996, **29**, 8934.
6 T. Kyu and J.-H. Lee, *Phys. Rev. Lett.*, 1996, **76**, 3746.
7 T. Ohnaga, W. Chen and T. Inoue, *Polymer*, 1994, **35**, 3774.
8 Z. Wang, Q. Ran, R. Zhu and Y. Gu, *J. Appl. Polym. Sci.*, 2013, **3**, 1124.
9 J. W. Park and S. C. Kim, *Polym. Adv. Technol.*, 1996, **7**, 209.
10 W. Gan, Y. Yu, M. Wang, Q. Tao and S. Li, *Macromolecules*, 2003, **36**, 7746.
11 Y. Yu, M. Wang, D. Foix and S. Li, *Ind. Eng. Chem. Res.*, 2008, **47**, 9361.
12 Y. Yu, M. Wang, W. Gan, Q. Tao and S. Li, *J. Phys. Chem. B*, 2004, **108**, 6208.
13 D. Feng, Y. G. Pei and X. X. Cai, *Acta Polym. Sin.*, 1998, **1**, 595.
14 J. E. White, *Ind. Eng. Chem. Prod. Res. Dev.*, 1986, **25**, 395.
15 Z. Shi, D. S. Yu, Y. Wang and R. Xu, *Eur. Polym. J.*, 2002, **38**, 727.
16 M. Rubinstein and R. H. Colby, *Polymer Physics*, Oxford University Press, New York, 2003.
17 J. H. Hildebrand, R. L. Scott, *Solubility of non-electrolytes*, Reinhold, New York, 3rd edn, 1950.
18 K. L. Hoy, *The Hoy tables of solubility parameters*, Union Carbide Corporation, South Charleston, WV, 1985.
19 Z. L. Zhang, H. D. Zhang, Y. L. Yang, I. Vinckier and H. M. Laun, *Macromolecules*, 2001, **34**, 1416.

